

Published in: Fütterer, D K, Damaske, D, Kleinschmidt, G, Miller, H & Tessensohn, F (eds.), *Antarctica: contributions to global earth sciences*, Springer, Berlin, Heidelberg, New York, 45-54
<http://dx.doi.org/10.1007/3-540-32934-X>

The original publication is available at <http://www.springerlink.com> see
http://dx.doi.org/10.1007/3-540-32934-X_6

Data are available at: <http://dx.doi.org/10.1594/PANGAEA.611560>

Genesis of Ferropotassic A-Type Granitoids of Mühlig-Hofmannfjella, Central Dronning Maud Land, East Antarctica

Mervin J. D'Souza · A. V. Keshava Prasad · Rasik Ravindra

Antarctica Division, Geological Survey of India, Faridabad, India, <antgsi@vsnl.net>

Abstract. Ferrosilite-fayalite bearing charnockite and biotite-hornblende bearing granite are exposed in Mühlig-Hofmannfjella, central Dronning Maud Land of East Antarctica. Both are interpreted as essentially parts of a single pluton in spite of their contrasting mineral assemblages. Based on petrologic and geochemical studies, it is proposed that H₂O-undersaturated parent magma with igneous crustal component that fractionated under different oxygen fugacity conditions resulted in the Mühlig-Hofmannfjella granitoids.

Introduction

Magmatic rocks associated with the Pan-African tectonic event form a large component of the lithological units exposed in central Dronning Maud Land (CDML). These magmatic rocks have been dated to represent an early Pan-African phase and a post-collisional late phase (Jacobs et al. 1998). The early intrusives (600 Ma) are the anorthosite massif exposed in the Grubergebirge and the Schüssel Mountains which was followed by granodiorites in Conradgebirge and charnockite-monzodiorite bodies of Wohlthat Massivet. The voluminous plutonic bodies exposed (Fig. 2.4-1a) in the Petermannketten (Joshi et al. 1991), the Conradgebirge and the Filchnerfjella have been dated at 530 to 510 Ma and they represent post-collisional A-type granitoids (Jacobs et al. 1998; Mikhalsky et al. 1995; Ravindra and Pandit 2000).

In the present study, the coarse undeformed granitoid exposed in Mühlig-Hofmannfjella (MH) forms the base for detailed geochemical and petrochemical studies in an attempt to characterize these rocks within the framework of dominant Pan-African magmatic activity recognized in the CDML.

Geological Outline

The geology of central Dronning Maud Land comprising the Wohlthatmassivet, Orvinfjella and the Mühlig-Hofmannfjella was first described by Ravich and Soloviev (1966) and Ravich and Kamanev (1972) and later by Indian and German geologists (Joshi et al. 1991; D'Souza et al.

1996; Bohrmann and Fritzsche 1995). Geological studies carried out in the area (Jacobs et al. 1998; Jacobs et al. 2003; Ohta et al. 1990; Paulsson and Austrheim 2003) has indicated that the exposed part of CDML has a very large component of Grenvillian (~1 000 Ma) crust which has been extensively modified during the Pan-African orogeny (600–500 Ma).

The oldest recognized rocks in CDML are the thick sequence of metaigneous and sedimentary rocks comprising banded orthogneiss, metapelites, metapsammities, calcsilicates, pyroxene granulites and amphibolites. The banded orthogneiss has been interpreted as representing a bimodal volcanic sequence. The basement rocks of CDML have indicated an earliest crystallization age of around 1 150–1 100 Ma (Jacobs et al. 2003) and high grade metamorphism between 1 090 and 1 050 Ma. The Grenvillian basement was later re-metamorphosed during the Pan-African orogeny associated with collision of East and West Gondwana around 550 Ma. (Jacobs et al. 1998; Markl et al. 2003). The Pan African orogeny in CDML is mainly represented as a prominent magmatic event which was activated before the collision with the intrusion of massif anorthosite. The magmatic activity apparently continued during the entire period and climaxed with the formation of post-collision extensional regime (530–510 Ma) which produced large volumes of granitic and syenitic rocks (Jacobs et al. 2003).

Field Description and Petrology

The Mühlig-Hofmannfjella granitoid pluton is exposed between. 71°30' to 6°30' S and 5°30' to 72°15' E (Fig. 2.4-1). These rocks are very coarse-grained, porphyritic and undeformed and are composed of K-feldspar (45–55%), quartz (30–35%), plagioclase (5–20%) and ferromagnesian minerals (up to 5%). The K-feldspar megacrysts measure up to 4 cm in length. The matrix is made up of plagioclase, quartz and ferromagnesian minerals. The rock having reddish colour has been distinguished as charnockite whereas the rock with whitish gray colour has been designated as granite. The granite and charnockite are seen to occur as patches on cliffs and slopes at several places and also in distinct zones demarcated by a horizontal line where the lower zone is of charnockite.

Restites of orthogneiss and charnockite (fine-grained, foliated) are very common. The proportion of restite was higher along the NE margin and the southern part of pluton and in the higher reaches of the pluton. The granitoids contain discrete shear zones.

The granitoid under the microscope is a heterogranular rock indicating compositional variation from granite/charnockite to granodiorite. Quartz occupying the interstitial space is comparatively less in the rocks. The reddish coloured charnockite and the granite show textural similarity and differ only by the presence of fayalite and ferrosilite in charnockite. The alkali feldspar is mesoperthitic orthoclase. The proportion of plagioclase in perthite greatly varies. Plagioclase occurs as interstitial mineral. The mesoperthite is often mantled by myrmekite comprising plagioclase and quartz. The mafic silicates and oxides occur as interstitial minerals. Biotite is mostly primary but also occurs as biotite-quartz symplectite rims around orthopyroxenes and amphiboles. Amphibole is anhedral, strongly pleochroic and green and brown in colour. In the charnockite, ferrosilite and fayalite are present in several thin sections studied but both these minerals are not observed in contact with each other. Inverted pigeonite is present in three samples. The accessory phases are mainly euhedral zircon, apatite, ilmenite and magnetite. Ilmenite is distinctly more abundant than magnetite. Fluorite specks were detected in two samples. Fayalite and ferrosilite frequently show alteration to amorphous Fe-silicate.

Mineral Chemistry

EPMA analysis were carried out using a CAMAECA-SX51 at the Geological Survey of India (GSI), Faridabad. Fayalite and ferrosilite are restricted to charnockite. The composition of fayalite is homogeneous at Fa_{94} and ferrosilite averages at Fs_{80-81} . In inverted pigeonite (Fig. 2.4-2), the ferrosilite (Fs_{78-80}) contains lamellae of ferroaugite ($Wo_{46}En_{16}Fs_{38}$). Amphibole is uniformly present in granites and charnockites. It is relatively iron-rich and is hastingsite in composition (Fig. 2.4-3).

Biotite is the most common ferromagnesian mineral present in MH granitoids. It is found as subhedral to anhedral grains and as secondary mineral around amphibole and pyroxenes. It is annite in composition. Alkali feldspar occurs as coarse porphyritic megacrysts and also as small grains. The alkali feldspar is orthoclase (Or_{84-90}) while that of the exsolved plagioclase lamellae is andesine (An_{33-39}). Plagioclase is also present in the matrix, which is oligoclase (An_{23-26}) in composition.

Geochemistry

Whole rock analyses were done using a Phillips XRF spectrometer at the Petrology, Petrochemistry and Ore Dressing (PPOD) laboratory, Airborne Mineral Survey and Exploration (AMSE) Wing, Geological Survey of India, Bangalore, and trace elements were analyzed using ICP-AAS at the Geological Survey of India, Faridabad. REE analysis was done using Instrumental NAA at the Geological Survey of India, Pune. Representative analysis of granitoids is given in Table 2.4-1. The representative analysis of restites occurring within the granitoids (Table 2.4-2) and the discrimination diagrams that follow suggest that the geochemical composition of enclave rocks compare well with that of host rock.

The MH granitoids are of monzogranite-quartz monzonite composition as indicated by a Qtz-Kfs-Plag plot (Fig. 2.4-4) based on molar norm (not given in the table) and they plot predominantly in metaluminous field in the A/NK versus A/CNK diagram (Fig. 2.4-5a). In TAS diagram of Middlemost (1997) the MH granitoids and associated enclaves show a transalkaline character (not shown). This is corroborated by the cationic classification *P-Q* diagram of Debon and Le Fort (1988). In this *P-Q* diagram, the MH samples show a distinct affinity to dark and light coloured subalkaline trend and plot in quartz syenite to granite field (Fig. 2.4-5b). In the K_2O versus SiO_2 (fields after Rickwood 1989) they plot in the shoshonitic field (Fig. 2.4-5c). The agpatatic index of these rocks is below 0.87 suggesting the rocks lack alkaline character (Fig. 2.4-5d).

On the cationic $Mg / Mg + Fe$ versus $Fe + Mg + Ti$ diagram of Debon and Le Fort (1988) the rocks show a strong ferriferous character (Fig. 2.4-5e). However due to high FeO/MgO ratios in the AFM diagram they plot in the tholeiitic field. In the $FeO/FeO+MgO$ versus SiO_2 and MALI diagram of Frost et al. (2001), the MH granitoids plot in the ferroan A-type granite field and alkali-calcic field respectively (Fig. 2.4-5f and 2.4-5g). The limited trace element data available with author shows a high content of HFSE like Nb, Zr and Ce and also incompatible elements like Ba and Sr. The tectonic discrimination diagrams for the MH granitoids obtained indicate WPG field (Fig. 2.4-5h) in the Nb versus Y diagram of Pearce et al. (1984) and a late orogenic and post collisional tectonic field (Fig. 2.4-5i) in the R1 versus R2 diagram of Bachelor and

Bowden (1985). Further these rocks have a high (La / Yb)_N ratio (Fig. 2.4-5j) suggesting a fractionated HREE/LREE trend.

Discussions

The MH granitoids exhibit a wide variation in the SiO₂ content varying from 59.03% to 75.89%. Based on their geochemical characteristics MH granitoids fit into a distinctive potassic group – A type granitoid (nomenclature after Loiselle and Wones 1979). These rocks have a high FeOt/FeOt + MgO ratio, high K₂O/Na₂O, comparatively low CaO and very low MgO concentrations. Moreover, the trace element data available indicate high contents of HFSE like Nb, Zr and Ce and incompatible elements like Ba and Sr. The presence of inverted pigeonite, high K, Ti P and low Ca, although indicate C-type magma affinity (Kilpatrick and Ellis 1992), very low MgO content and presence of modal fayalite preclude these rocks from the C type charnockites. Further, the MH Pluton is transalkaline ferroan A-type granite, which concurs well with the observation of Frost et al. (2001) that world over the A-type granitoids are overwhelmingly ferroan alkali calcic to calcic-alkali in character.

The SiO₂ content of MH granitoids varies from 59.03% to 75.89%. This variation is reflected by consistent conformable trend in Harker diagram for CaO, MgO, FeOt and TiO₂ as their amount increases with decrease in SiO₂ content (plots not shown). The granite and charnockite plots overlap each other in the Harker diagram suggesting both these rocks to be part of a single pluton and have fractionated from same source. This is also confirmed by the visible textural conformity between granite and charnockites in the outcrops.

Based on the mineral assemblage of charnockite and granite, available geochemical data and a comparison with other ferropotassic A-type granites (Bogaerts et al. 2003; Guimarões et al. 2000; Ferré et al. 1998; Roland 1999) an anhydrous to H₂O-undersaturated parent magma with igneous crustal component is considered as a possible source for the MH granitoids. The involvement of igneous crustal source in the generation of magma is considered to accommodate the transalkaline, potassic and ferriferous character of these rocks. The restitic enclaves like diorite, charnockite (occurring within the granitoids as enclaves) with low SiO₂, high K₂O and FeOt/FeOt + MgO and having composition akin to ferro-monzonite and or ferro-monzodiorite may possibly represent the crustal component in the source magma. Melting of such igneous crustal components must have occurred at high temperature and very low, near-constant oxygen fugacity to crystallize ferrosilite and fayalite in the beginning. As the magma slowly cooled and moved towards shallower depths, it underwent fractional crystallization. During this process, according the Bucher and Frost (1993), the melt can attain water saturation. The resultant increase in the oxygen fugacity facilitated crystallization of ilmenite and magnetite instead of ferrosilite and fayalite. This possibly explains an important observation (made during mineral separation process) that the volume of magnetic minerals (mainly ilmenite and magnetite) present in charnockite is far less compared to that in the granite. The increased H₂O-activity was conducive for the formation of biotite-hornblende bearing granitic assemblage and retrogression of part of the early-crystallized pluton in patches and zones. Thus the charnockite containing fayalite and ferrosilite represents the early-crystallized phase of MH Pluton.

Conclusion

The field disposition of the MH granitoids is very much similar to the Svarthmaren charnockite occurring in western Mühlig-Hoffmanfjella, which has been dated at 500 ± 24 Ma by Ohta et al. (1990). Geochemically, the MH granitoids compare very well with similar transalkaline ferro-potassic A-type Pan-African granitoids reported from Nigeria and Brazil (Ferre et al. 1998; Guimaraés et al. 2000) and to some extent with Pan-African A-type granitoid reported from Kerala Khondalite Belt, India, Madagascar and the Arabian-Nubian Shield (Rajesh 2000; Moghazi 2002; Nédélec et al. 1995). The magmatism associated with Pan-African orogeny in CDML is linked to the continent-continent collision involving east and west Gondwana in the final assembly of Gondwana. This orogenic cycle that started with the intrusion of anorthosite at 600 Ma (Bauer et al. 2002) progressed through continent-continent convergence and metamorphism at 580–560 Ma. The second phase of metamorphism interpreted at 530–510 Ma, was associated with an extensional regime causing intrusion of voluminous granitoids in the area (Jacobs et al. 2003). The MH granitoids, in absence of any deformational or metamorphic feature, is considered to be post-tectonic/post-collisional. The within-plate feature shown by Nb *versus* Y tectonic discrimination diagram and the post-collision/late orogenic feature reflected by the R_1 - R_2 diagram (Fig. 2.4-5h and 2.4-5i) conform to this conclusion. The continent – continent convergence led to thickening of the crust followed by collapse of the subducted, predominantly igneous, crust that was involved in the formation of melt giving rise to MH granitoids.

Acknowledgments

This publication is the result of work carried out during the 20th Indian Antarctic Expedition conducted under the aegis of National Center for Antarctic and Ocean Research (NCAOR), Goa, India. The authors wish to acknowledge the co-operation extended by colleagues Jayapaul D. and Dharwadkar A. Critical reviews by Norbert Roland and Hartwig Frimmel have considerably helped to improve this contribution.

References

- Bachelor RA, Bowden P (1985) Petrologic interpretation of granitoid rock series using multicationic parameters. *Chem Geol* 48:43–55
- Bauer W, Thomas RJ, Jacobs J (2002) Proterozoic-Cambrian history of Dronning Maud Land in context of Gondwana assembly. In: Windly BF, Dasgupta S (eds) *Proterozoic East Gondwana: supercontinent assembly and breakup*. *Geol Soc London* 206:247–269
- Bogaerts M, Scaillet B, Liégeois J, Auwera JV (2003) Petrology and geochemistry of the Lyngdal granodiorite (southern Norway) and the role of fractional crystallization in the genesis of Proterozoic ferro-potassic A-type granites. *Precamb Res* 124:149–184
- Bohrmann P, Fritzsche D (1995) The Schirmacher Oasis, Queen Maud Land, East Antarctica and its surroundings. *Petermanns Geograph Mitt Ergänzungsheft* 289, Justus Perthes, Gotha
- Bucher K, Frost BR (1993) Crystallization history of charnockites, Thor range and implication to thermobarometry of cordierite gneisses (abstract). *Geol Soc Amer Abst Program* 25:448

- D'Souza, MJ, Kundu A, Kaul MK (1996) The geology of central Dronning Maud Land (cDML), East Antarctica. *Ind Min* 50:323–338
- Debon F, Le Fort P (1988) A cationic classification of common plutonic rocks and their magmatic associations: principles, method application. *Bull de Minéralogie* 111:493–510
- Ferré EC, Caby R, Peucat JJ, Capdevilla R, Monie P (1998) Pan-African, post-collisional, ferro-potassic granite and quartz-monzonite plutons of eastern Nigeria. *Lithos* 45:255–279
- Frost BR, Barnes CG, Collins WJ, Arculus RJ, Ellis DJ, Frost CD (2001) A geochemical classification for granitic rocks. *J Petrol* 42:2033–2048
- Guimarães IP, Almeida CN, Filho AFD, Araújo JM (2000) Granitoids marking the end of the Brasiliano (Pan-African) orogeny within the central tectonic domain of the Borborema Province. *Revista Brasileira Geociencias* 30:177–181
- Jacobs J, Fanning CM, Henjes-Kunst F, Olesch M, Paech H-J (1998) Continuation of the Mozambique Belt into East Antarctica: Grenville-Age metamorphism and polyphase Pan-African high grade events in central Dronning Maud Land. *J Geol* 106:385–406
- Jacobs J, Baur W, Fanning CM (2003) Late Neoproterozoic/Early Palaeozoic events in central Dronning Maud Land and significance for the southern extension of the East African Orogen into East Antarctica. *Precam Res* 126:27–53
- Joshi A, Pant NC, Parimoo ML (1991) Granites of Petermann ranges, east Antarctica and implication on their genesis. *J Geo Soc Ind* 38:169–181
- Kilpatrick JA, Ellis DJ (1992) C-type magmas: igneous charnockites and their extrusive equivalents. *Trans Royal Soc Edinburgh Earth Sci* 83:155–164
- Leake B (1978) Nomenclature of amphiboles. *Can Miner* 16:501–520
- Le Maitre RW (1989) A classification of igneous rocks and glossary of terms. Recommendations of the International Union of Geological Sciences. Subcommission on the Systematics of Igneous Rocks, 1st edn. Blackwell, Oxford
- Liégeois J-P, Black R (1987) Alkaline magmatism subsequent to collision in the Pan-African belt of the Adrar des Iforas. In: Fitton JG, Upton BGJ (eds) *Alkaline igneous rocks*. Geol Soc, Blackwell Scientific, Oxford, pp 381–401
- Loiselle MC, Wones DR (1979) Characteristics and origin of anorogenic granites. *Geol Soc Amer Abstr Program* 11:468
- Maniar PD, Piccoli PM (1989) Tectonic discrimination of granitoids. *Geol Soc Amer Bull* 101:635–643
- Markl G, Abart R, Vennemann T, Sommer H (2003) Mid-crustal metasomatic reaction veins in a spinel peridotite. *J Petrol* 44:1097–1120
- Middlemost EAK (1997) *Magmas rocks and planetary development*. Longman, Harlow
- Mikhalsky EV, Grikurov GE (2003) East Antarctica crust growth from the isotopic data (abstract). 9th Int. Sympos Antarctic. Earth Science, Terra Nostra 2003(4):230–231
- Mikhalsky EV, Beliatsky BV, Savva EV, Federov LV, Hahne K (1995) Isotopic systematics and evolution of metamorphic rocks from the northern Humboldt Mountains, the Queen Maud Land, east Antarctica (abstract). VII Internat Sympos Antarctic Earth Sci, Siena
- Moghazi AM (2002) Petrology and geochemistry of Pan-African granitoids, Kab Amiri area, Egypt-implications for tectonomagmatic stages in the Nubian Shield evolution. *Mineral Petrol* 75:41–67
- Nakamura N (1977) Determination of REE, Ba, Fe, Mg, Na and K in carbonaceous and ordinary chondrites. *Geochem Cosmochim Acta* 38:757–775

- Nédélec A, Stephens WE, Fallick AE (1995) The Pan-African stratoid granites of Madagascar: alkaline Magmatism in post-collisional extensional setting. *J Petrol* 36:1367–1391
- Ohta Y, Tørudbakken Bo, Shiraishi K (1990) Geology of Gjelsvikfjella and western Mühlig-Hofmannfjella, Dronning Maud Land, East Antarctica. *Polar Res* 8:538–544
- Paulsson O, Austrheim H (2003) A geochronological and geochemical study of rocks from Gjelsvikfjella, Dronning Maud Land, Antarctica – implications for Mesoproterozoic correlations and assembly of Gondwana. *Precambrian Res* 125:113–138
- Pearce JA, Harris NB, Tindle AG (1984) Trace element discrimination diagrams for the tectonic interpretation of granitic rocks. *J Petrol* 25:956–983
- Rajesh HM (2000) Characterization and origin of a compositionally zoned aluminous A-type granite from South India. *Geol Mag* 137:291–318
- Ravich MG, Kamenev EN (1972) Crystalline basement of the Antarctic platform. (1st English edn. 1975, Wiley, New York)
- Ravich MG, Soloviev DS (1966) Geology and petrology of the mountains of Central Dronning Maud Land (eastern Antarctica). *Trans Sci Res Inst Arctic Geol, Ministry of Geology* (transl. in Jerusalem, 1969)
- Ravindra R, Pandit MK (2000) Geochemistry and geochronology of A-type granite from northern Humboldt Mountains, East Antarctica: Vestige of Pan-African event. *J Geol Soc India* 56:253–262
- Rickwood PC (1989) Boundary lines within petrologic diagrams, which use oxides of major and minor elements. *Lithos* 22:247–264
- Roland N (1999) Pan-African granitoids in central Dronning Maud Land, East Antarctica. Petrography, geochemistry and their plate tectonic setting. In: Skinner DNB (ed) *Programme and abstract 8th Internat Sympos Antarctic Earth Sci*

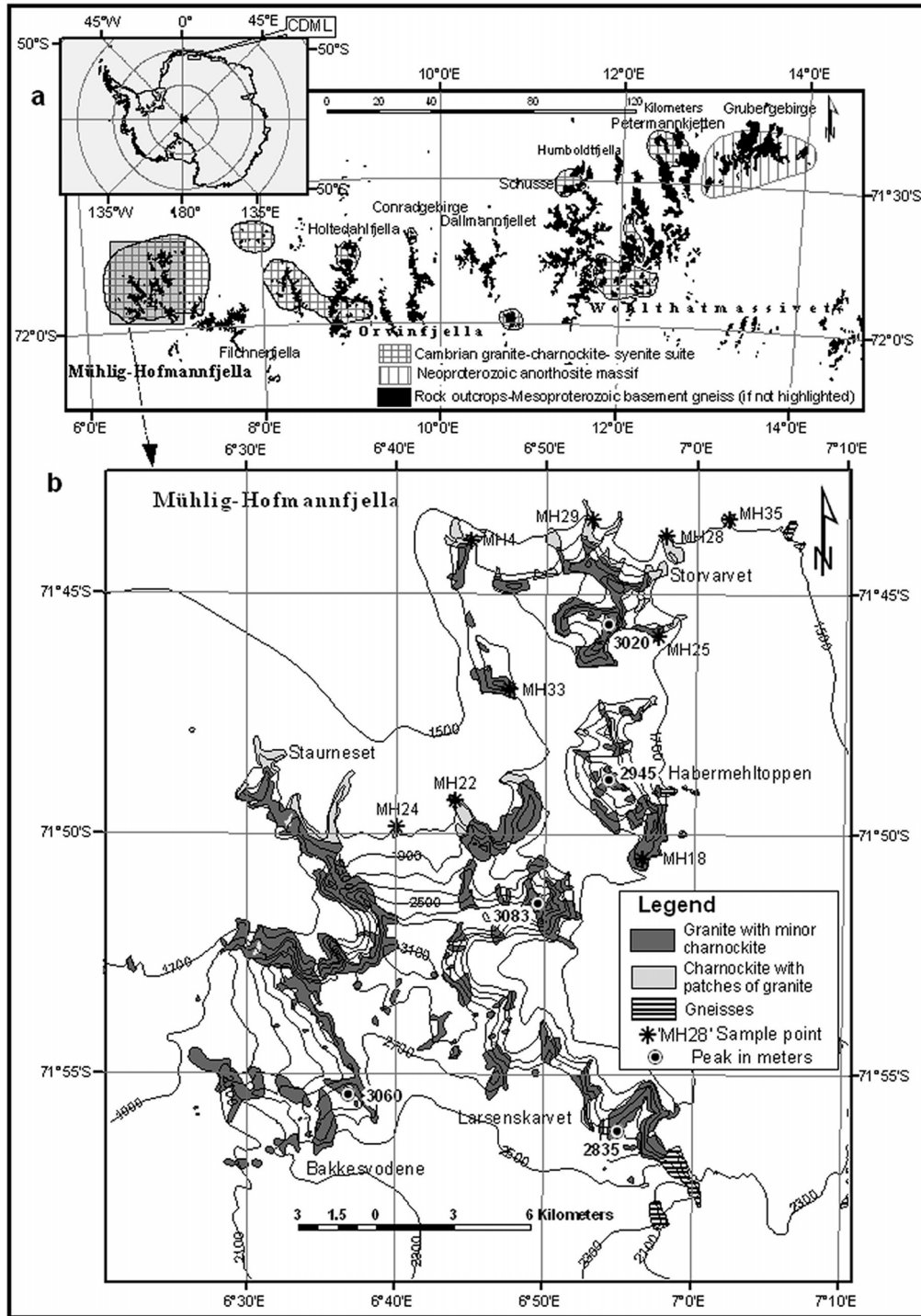


Fig. 2.4-1. a Lay out of outcrops in central Dronning Maud Land, East Antarctica, showing distribution of granite-charnockite-syenite plutons, anorthosite massif and the basement gneisses. **b** Geological Map of eastern Mühlig-Hofmannfjella with sample locations

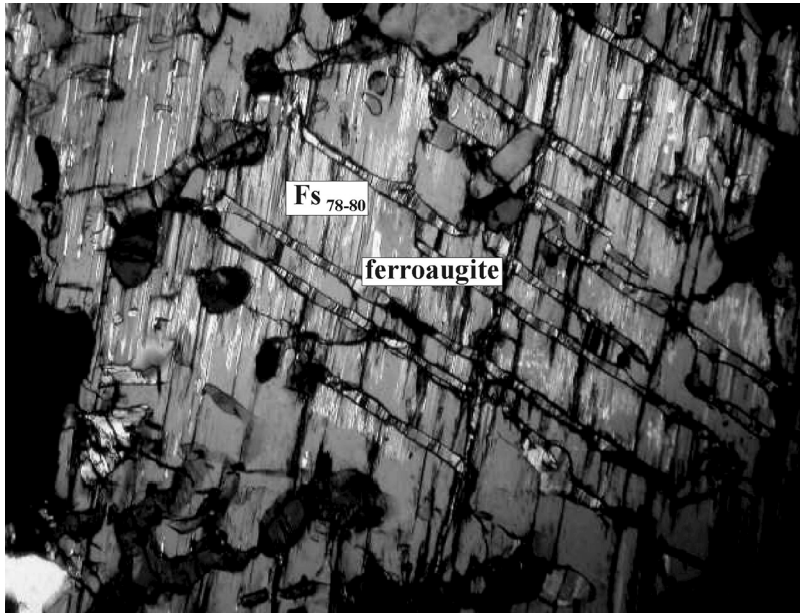


Fig. 2.4-2.
Inverted pigeonite with ferroaugite lamellae in a sample of charnockite from Mühlig-Hofmannfjella area (MH 28)

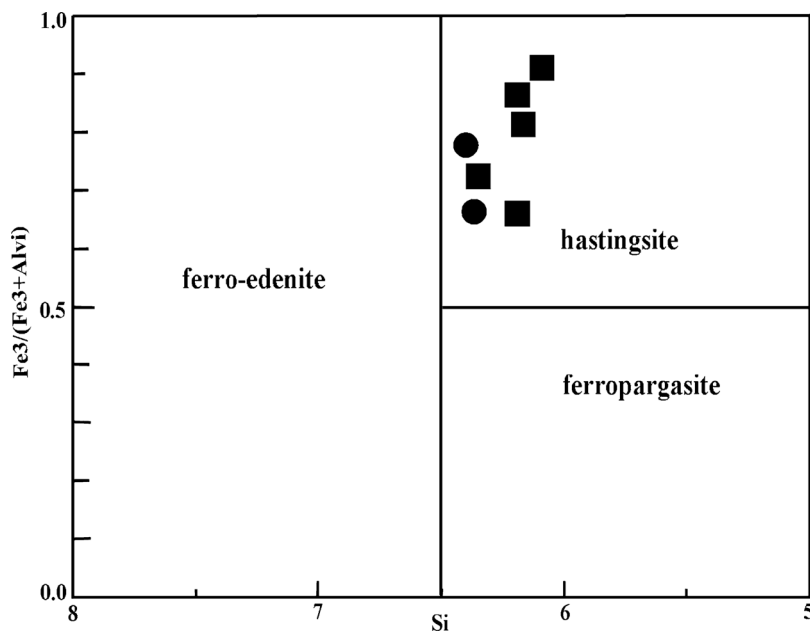


Fig. 2.4-3. Fe³⁺/(Fe³⁺ + Al_{vi}) versus Si in formula unit diagram for classification of amphibole (Leake 1978). Symbols shown are common for all ensuing diagrams in the manuscript

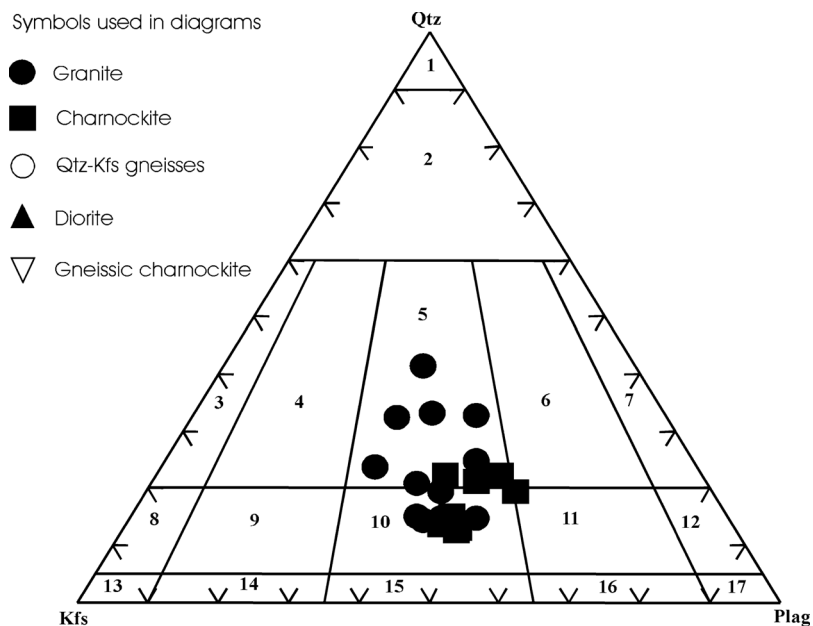


Fig. 2.4-4.

Modal composition *Qtz-Kfs-Plag* ternary diagram of Mühlig-Hofmann (MH) granitoids and enclaves plot in monzo granite and quartz monzonite fields. The fields of plutonic rocks after Le Maitre (1989): 1: Quartzolite; 2: Qtz rich granite; 3: Qtz-Kfs granite; 4: syeno granite; 5: monzo granite; 6: granodiorite; 7: tonalite; 8: Qtz-Kfs syenite; 9: Qtzsyenite; 10: Qtz-monzonite; 11: qtzmonzodiorite; 12: Qtz-diorite; 13: Kfssyenite; 14: syenite; 15: monzonite

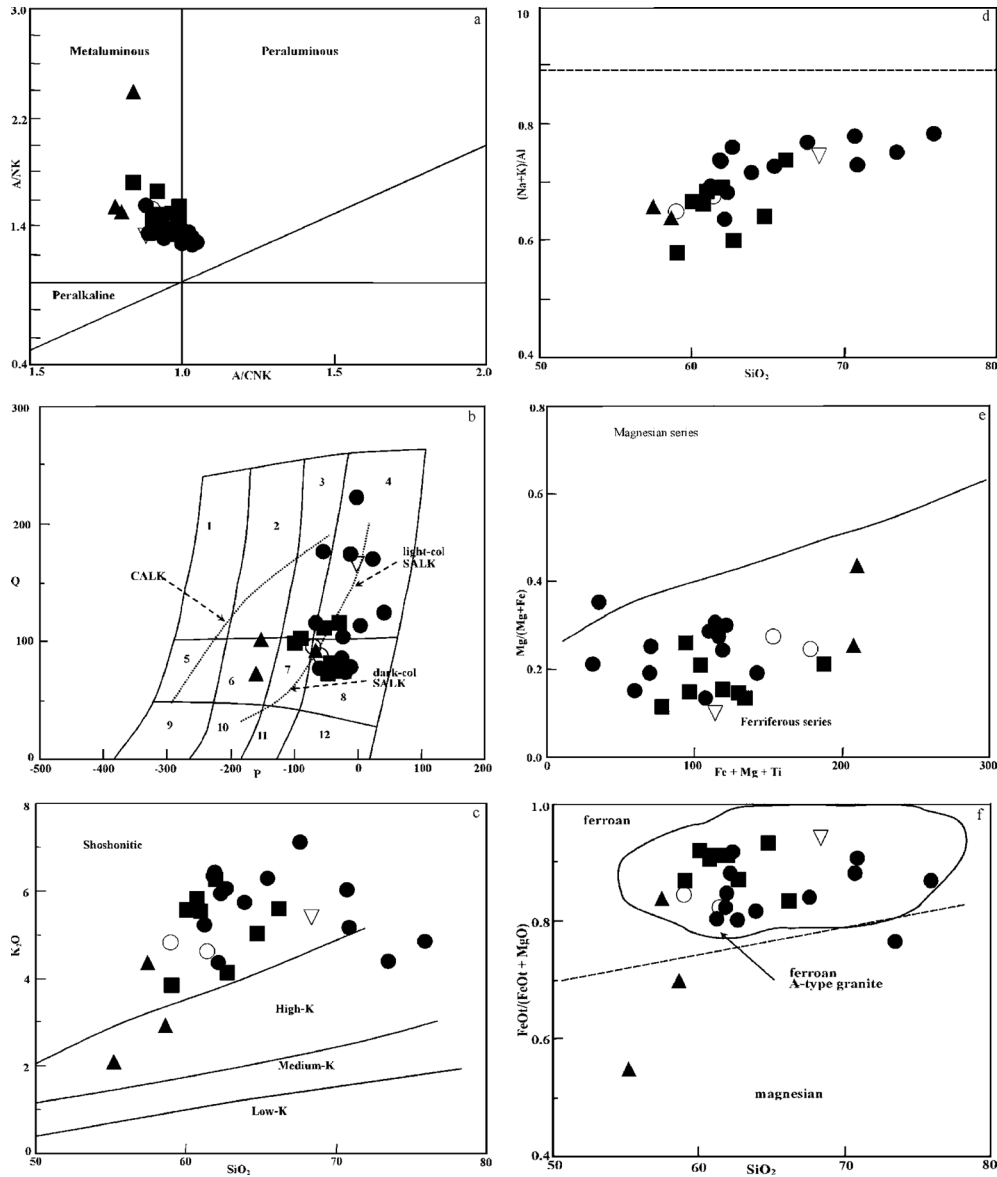


Fig. 2.4-5a-f. **a** Dominantly metaluminous character of Mühlig-Hofmann (MH) granitoids (Shands molar parameters after Maniar and Piccoli (1989)). **b** Cationic classification of Debon and Le Fort (1988): $Q = Si/3 - (K + Na + 2Ca/3)$ versus $P = K - (Na + Ca)$; shown subalkaline (SALK) trend and calc-alkaline (CALK) trends: 1: tonalite; 2: granodiorite; 3: adamellite; 4: granite; 5: Qtz-diorite; 6: Qtz-monodiorite; 7: Qtz-monzonite; 8: Qtz-syenite; 9: gabbro or diorite; 10: monodiorite; 11: monzonite; 12: syenite. **c** K_2O versus SiO_2 (wt.-%) diagram, the limits given are after Rickwood (1989). **d** Agpaitic index (molar $(Na/K)/Al$ versus SiO_2). The limit at 0.87 separates subalkaline metaluminous granitoids from alkaline (Liégeois and Black 1987). **e** Ferriferous character in $M = Mg/(Mg + Fe)$ versus $B = Fe + Mg + Ti$ in cationic classification diagram after Debon and Le Fort (1988). **f** $FeO/(FeO + MgO)$ versus SiO_2 showing boundary between Ferroan and magnesian granitoids. The A-type granitoid boundary based on 175 samples after Frost et al. (2001)

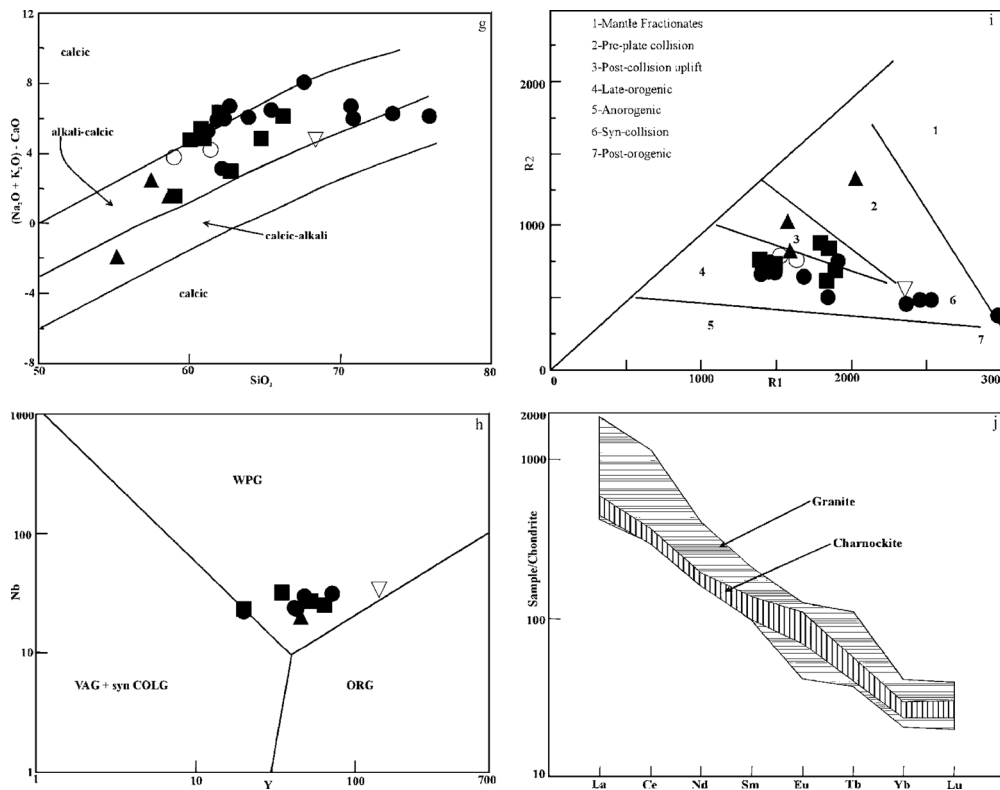


Fig. 2.4-5g–j. **g** Na₂O+ K₂O – CaO versus SiO₂ plot after Frost et al. (2001), showing ranges for alkali, alkali-calcic, calcic-alkali and calcic fields. **h** Trace element tectonic discrimination diagram Nb versus Y after Pearce et al. (1984). **i** R1-R2 diagram after Bachelor and Bowden (1985). **j** Chondrite normalised REE spidergram. Normalising values after Nakamura (1977)

Table 2.4-1 Whole rock and trace element analysis of MH granitoids; analysis of major oxides using XRF, analysis of trace elements using ICP

Table 2.4-2 Whole rock and trace element analysis of representative enclave rocks occurring within MH granitoids

Table 2.4-3 REE analysis by instrumental NAA of MH granitoids

Data tables are available at doi:[10.1594/PANGAEA.611560](https://doi.org/10.1594/PANGAEA.611560)